Photoemission and X-ray Absorption Study of the Interface between 3,4-Ethylenedioxythiophene-Related Derivatives and Gold

ARTICLE *in* THE JOURNAL OF PHYSICAL CHEMISTRY C · JULY 2012

Impact Factor: 4.77 · DOI: 10.1021/jp304758b

4 AUTHORS, INCLUDING:

Luca Pasquali
Università degli Studi di Modena e Reggio Emilia
101 PUBLICATIONS **1,056** CITATIONS
SEE PROFILE

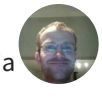

B. P. Doyle
University of Johannesburg
77 PUBLICATIONS **799** CITATIONS
SEE PROFILE

Renato Seeber
Università degli Studi di Modena e Reggio Emilia
211 PUBLICATIONS **2,804** CITATIONS
SEE PROFILE

THE JOURNAL OF PHYSICAL CHEMISTRY C

Article

pubs.acs.org/JPCC

Photoemission and X-ray Absorption Study of the Interface between 3,4-Ethylenedioxythiophene-Related Derivatives and Gold

Luca Pasquali,*[,†,‡] Fabio Terzi,[§] Bryan P. Doyle,[⊥] and Renato Seeber[§]

[†]Department of Materials and Environmental Engineering, University of Modena and Reggio Emilia, Via Vignolese 905, 41125 Modena, Italy

[‡]IOM-CNR,Area Science Park , Basovizza, s.s.14, km 163.5, 34149, Trieste, Italy

[§]Department of Chemistry, University of Modena and Reggio Emilia, Via Campi 183, 41125, Modena, Italy

[⊥]Department of Physics, University of Johannesburg, PO Box 524, Auckland Park, 2006, South Africa

ABSTRACT: The chemisorption of 3,4-ethylenedioxythiophene (EDOT) derivatives on Au(111) single crystal and polycrystalline surfaces is studied with valence band photoemission and near edge X-ray absorption fine structure (NEXAFS) spectroscopy. Different EDOT derivatives are considered, namely EDOT itself, its dimer (bi-EDOT), 3′,4′-ethylenedioxy-2,2′:5′,2″-terthiophene (TET) and some of the relevant electro-generated polymers, being PEDOT at different stages of substrate coverage and the TET polymer. The interpretation of the valence band spectra is carried out by comparing with DFT calculations of the densities of states of different possible reaction products that can be formed at the interface. Simulation of the NEXAFS spectra of EDOT and thiophene and comparison with literature data on thiophene and oligothiophene films are used for the interpretation of the X-ray absorption spectra of bi-EDOT, TET on Au, and the TET polymer and PEDOT at different electro-polymerization times. Valence band features that are associated to EDOT products are identified together with new structures that are ascribed to reactive dissociation products at the interface. In particular the presence of unsubstituted thiophene/oligothiophene molecules is observed, together with possible alkyl chains. NEXAFS indicates that the thiophene rings tend to adopt a planar configuration at the interface.

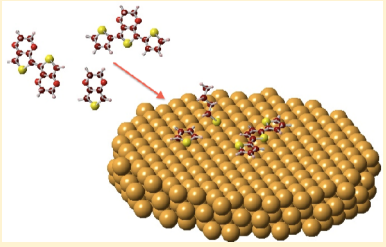

INTRODUCTION

In organic−inorganic hybrid systems, a crucial role is played by the interface between the two materials. Adhesion, self-assembly, molecular ordering, and chemical reactions between organic and inorganic constituents can deeply influence the overall performance, both electrical and mechanical, of the related devices.[1−4] In molecular electronics, the interface between the organic semiconductors (either molecular or polymeric films) and metal electrodes is critical for the electronic level alignment and for the determination of charge injection barriers.[5,6]

Most detailed studies in the literature have been dedicated to the interface properties of ultrathin films of thiol-derived molecules on metal surfaces.[7−13] It has been shown in differing circumstances that the growth mode and interface properties of the molecular layer can be deeply influenced by a proper choice of the preparation conditions.[14−18]

The interface properties of thiophene derivatives with metals are much less investigated, in spite of their extensive application in molecular electronics as well as in (electrochemical) sensing. Thiophene derivatives are used either in the form of thin molecular films or polymeric layers, depending on the type of device and field of application.[19−21] In most cases, the interest is principally focused on the bulk properties of the organic material. Even in the simplest cases, i.e., small thiophene-derived molecules chemisorbed on Au substrates, an overall consensus on the interface characteristics has not been reached. This is related to the different preparation conditions adopted in different studies, principally depending on the deposition method, consisting either of evaporation in vacuum or of film formation in solution.[22−28] The cleanliness of the substrate prior to deposition is also extremely important.[5,6]

We have recently investigated the interface properties of 3,4-ethylenedioxythiophene (EDOT) and some of its derivatives on Au.[29,30] Au was chosen as it represents one of the most widely used electrodes in organic electronics and in (electrochemical) sensing. In turn PEDOT, the relevant polymer derived from EDOT, is known to present particularly appealing properties for technological applications, such as high stability, high electrical conductivity, low oxidation potential and optical transparency in the visible range.[31,32] Applications of PEDOT include light emitting diodes, organic thin film transistors, electroluminescent devices, capacitors, antistatic coatings, solar cells, and sensors.

The interface between the two materials was expected to be inert and stable, due to the stability of the constituents. However, contrary to expectations, it was found that the noble metal Au is not inert toward EDOT. Electron[29,30] and vibrational[29] spectroscopies demonstrated that EDOT and some of its relevant derivatives, namely the dimer (bi-EDOT),

Received: May 16, 2012
Revised: June 22, 2012
Published: June 22, 2012

   dx.doi.org/10.1021/jp304758b | J. Phys. Chem. C 2012, 116, 15010−15018

3′,4′-ethylenedioxy-2,2′:5′,2″-terthiophene (TET) and PEDOT at the initial electro-generation stage, tend to decompose at the Au surface, leading to the scission of the $C_{aromatic}$−O bonds and to the possible formation of oligothiophenes and alkanethiolates. The reaction was demonstrated to be independent of the deposition method, either in solution or by evaporation in vacuum, and it was observed on different types of Au substrates, namely single crystal, polycrystalline surfaces and Au nanoparticles.

This work extends our previous investigation. The valence bands of EDOT, bi-EDOT, TET on Au, and the electrogenerated PEDOT and TET polymer are presented, as measured by photoemission spectroscopy. The spectral line shape is discussed by comparing the experiment with the calculated density of states (DOS) of the different molecules and possible interface reaction products. NEXAFS spectra at the carbon C 1s level are also studied for the case of bi-EDOT and TET on Au(111), for a TET polymer film and for the electrogenerated PEDOT film. Results are discussed on the basis of the comparison with literature and with calculated X-ray absorption spectra. The data collected confirm the reactive dissociation picture for all the investigated molecular films at the interface with Au and support the idea of an interface layer composed of single thiophene units or oligothiophenes and alkyl chains as reaction products.

EXPERIMENTAL METHODS

The experimental procedure was the same as the one reported in ref 29. Two different types of planar substrates were used, namely commercial Au polycrystalline films (200 nm thick), grown on a flat glass support coated by a 2 nm thick Cr buffer layer (Universal Sensors), and a Au(111) single crystal (Mateck).

All chemicals were from Aldrich, except for TET, which was synthesized according to ref 33.

The polycrystalline substrates were cleaned with a piranha solution before immersion into a 10 mM EDOT aqueous solution. The vessels used for the film preparation were stored at room temperature in darkness. The resulting EDOT films were rinsed in ultrapure water after removal from the solution, and quickly inserted into the ultra high vacuum (UHV) chamber for analysis.

The single crystal surface was cleaned by cycles of sputtering (Ar^+ ions at 500 eV) and annealing (at 400 °C). Ca. 1 g of EDOT, bi-EDOT, or TET were inserted into a vacuum-sealed glass tube connected to the UHV chamber through a leak valve. Several pumping cycles were applied before exposure of the clean Au surface to the molecular vapors. Exposure was accomplished in a small vacuum chamber preliminarily saturated with the thiophene derivative. The glass tube containing the EDOT vapors was kept at room temperature during exposure while, in the case of bi-EDOT and TET, the tube was heated to 115 °C. The substrate was kept at room temperature during all exposures. Due to the low sticking efficiency of thiophene derivatives at the Au surface[23] during vapor deposition, exposures at doses as high as 10^5 L were adopted.

PEDOT and TET polymer thin films were electro-generated under galvanostatic conditions (0.4 mA·cm^{-2} current density) from a 10 mM monomer solution containing 0.1 M $NaBF_4$ as supporting electrolyte. Water and dichloromethane have been chosen as solvents for EDOT and TET, respectively. Polycrystalline Au substrates similar to those used for the deposition of EDOT from the aqueous phase were used. Different polymerization times were employed, namely 0.03, 0.06, 0.25, 1, 3, 10, and 160 s. After the polymerization, the thin films were thoroughly rinsed with ultrapure water and dried in air. In order to verify if the adsorbed layer is desorbed during the first instants of the PEDOT electro-generation process, an Au polycrystalline electrode was dipped for 5 min in a 10 mM EDOT aqueous solution containing 0.1 M $NaBF_4$. The electrode was then removed from the EDOT solution, thoroughly rinsed with ultrapure water and inserted in an electrochemical cell containing only the supporting electrolyte. A +1.0 V potential step was applied for 10 s. Finally, the electrode was thoroughly rinsed with ultrapure water and dried in air.

Photoemission and X-ray absorption experiments were performed in the UHV end station of the BEAR beamline at the ELETTRA synchrotron radiation laboratory.[34,35] Photoemission measurements from the valence band were performed at normal emission with a hemispherical deflection analyzer (66 mm mean radius) driven at constant pass energy, with 100 meV energy resolution. The photon energy was 60 eV for all investigated samples. The incident angle was 45°. Photoemission core level spectra from the substrate and overlayers were acquired within the same runs and reported elsewhere.[29] Au 4f emission from the substrate was used to evaluate the organic layer *effective* thickness, assuming a standard exponential attenuation of the signal and a uniform coverage. The Au 4f levels were measured at 185 eV of photon energy, estimating a value of 6 Å for the inelastic mean free path.[30]

NEXAFS was measured by scanning the photon energy in correspondence to the C 1s absorption edge. Spectra were acquired with linearly polarized light (degree of linear polarization P = 0.94), in s- and p- scattering conditions, with a grazing incident angle of 20° with respect to the sample plane. The energy resolution was 0.1 eV. To enhance surface sensitivity, the spectra were acquired in Auger electron yield mode, by monitoring the carbon Auger signal intensity as a function of the photon energy. Total yield acquisition mode was used for the TET polymeric film. To correct for beam flux variations and optics transmission, the spectra were first normalized to the current drained by a gold mesh (flux monitor) and then further normalized to a reference spectrum acquired on a carbon-free Au surface. Characteristic features of the flux monitor signals were used to align the energy scales of the spectra. All measurements were performed at room temperature.

COMPUTATIONAL METHODS

The DOS of different thiophene derivatives (isolated molecules), ranging from simple thiophene to the EDOT trimer (Figures 1−3), and of butanethiol were calculated by DFT with the quantum chemistry code StoBe.[36] A gradient-corrected RPBE exchange/correlation functional was used.[37,38] The equilibrium geometry and the valence band properties of the molecules were obtained using double-ζ valence basis sets (triple-ζ for EDOT and thiophene) including polarization functions.[39]

The carbon NEXFAS spectra of EDOT and thiophene were calculated applying the Slater transition state method.[40,41] The geometry-optimized molecular structure computed for the ground state was kept fixed and dipole transitions were calculated at all nonequivalent C atomic centers. We used an IGLO-III basis on each excitation center to achieve a better

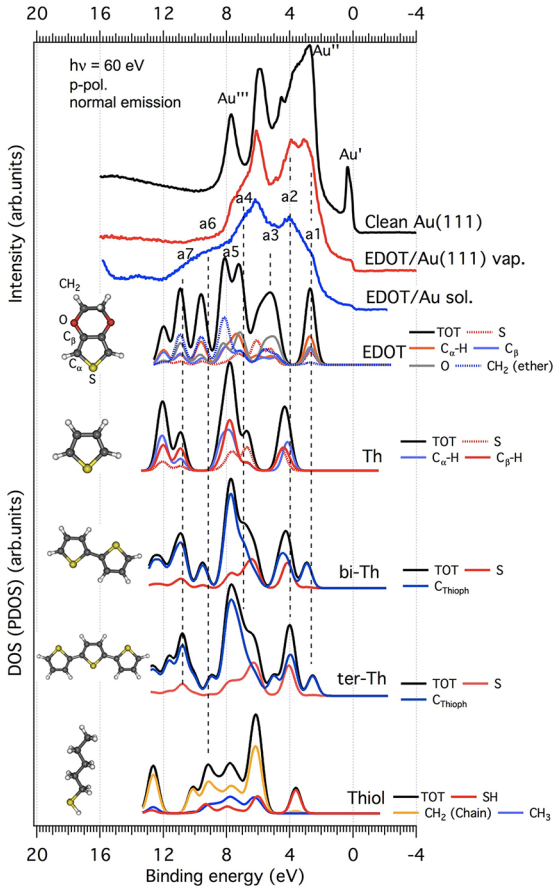

Figure 1. Valence band of clean Au(111) and EDOT/Au films prepared from vapor deposition and by dipping in solution. The DOS of EDOT, thiophene, bithiophene, terthiophene, and butanethiol are reported. PDOS projected onto specific molecular groups are indicated.

description of the relaxation effects, while for the remaining carbon atoms we used effective core potentials (ECP) describing the core and the appropriate valence basis.[36] A large diffuse basis set was finally included at the excitation center to account for transitions to unbound resonances and continuum states. The dipole-excitation spectra obtained in this way were then Gaussian-convoluted with an energy dependent broadening. Before comparison with the experiment, for a correct energy scale alignment of the spectra of nonequivalent centers, an additional ΔKohn−Sham adjustment[42,43] to the lowest core-excited state for each center was applied.

RESULTS

Valence Band Photoelectron Spectroscopy. The electron distribution curves of the valence bands for different EDOT-derived films on Au are reported in Figures 1−3. The spectra are referenced to the Fermi level. In the same figures the DOS of different molecules that can be expected to be possible reaction products of the chemisorption reaction, are also shown. The experimental valence bands of Figures 1−3 refer to the same systems already discussed in ref 29.

In Figure 1 the valence band spectra of EDOT deposited in solution and from the vapor phase are compared.[30] The spectrum of the clean single crystal is also shown, to highlight the experimental features due to the clean Au(111) substrate. In particular, well-pronounced surface states (Au′, Au″, and Au‴)[44,45] are visible, together with prominent structures, which are assigned to the Au 5d band, dominating the electron distribution curve between 2.5 and 8 eV. While chemisorption from the vapor phase was performed directly on the Au(111) single crystal surface, EDOT deposition from solution was carried out on a polycrystalline surface. In this case, a representative curve for the clean substrate is shown as the top spectrum in Figure 3. The surface state right below the Fermi energy (Au′) and the Au″ and Au‴ states are not distinguishable and the spectrum is dominated by emission from the Au 5d band.

EDOT chemisorption, either from vapor or from solution, induces an overall smearing out of the Au features, with a complete quenching of the surface states of Au(111). The spectra are still dominated by emission from the Au 5d band, although new features appear, the most intense ones being labeled from a1 to a7 in Figure 1. In the EDOT film prepared in solution the attenuation of the substrate features is more marked, consistent with a higher *effective* thickness of the organic layer. From the attenuation of the Au 4f levels, the *effective* thickness was evaluated to be of the order of 3 and 2 Å for the films prepared in solution and from the vapor phase, respectively.[30] Features above 8 eV binding energy are also more pronounced.

Also in Figure 1, below the experimental spectra, the calculated DOS of several molecules are reported that can be envisaged as the possible molecular species or fragments that remain at the surface after chemisorption. These include EDOT, thiophene (Th), thiophene dimer and trimer (bi-Th and ter-Th), and butanethiol. For each molecule, the partial densities of states (PDOS) projected on specific sites or molecular groups are also shown, to facilitate the assignation of the different features to particular molecular units.

For comparison purposes, the DOS curves were aligned on the energy scale in consistency with the experimental works of Birgerson et al.[46] and Osikowicz et al.[47,48] for EDOT and its oligomers (see Figures 2 and 3), with the works of Chandekar et al.[49] and Fujimoto et al.[50] for thiophene, its dimer and trimer, and with the works of Duwez et al.[12,51,52] for thiol.

In Figure 2, the valence band electron distribution curves of the EDOT dimer (bi-EDOT) and of the TET monomer films from vapor deposition on Au(111) are compared to the curve obtained on a thick polymeric TET film on Au (TET poly). After chemisorption the spectra of TET and bi-EDOT are quite similar. Also in this case the surface states of Au are quenched, although some survival of the Au′−Au‴ features is observed for the TET case. Attenuation of the Au 4f core levels was used to estimate an *effective* thickness of 6 and 2 Å for the bi-EDOT and the TET monomer films, respectively. New features due to the adsorbates are not pronounced, especially for the TET monomer, the only contributions being observed at about 4 eV (b3) and above 8 eV. Some weaker shoulder can be noticed at about 2 eV below the Fermi level. Concerning the TET polymer curve, the contributions from the substrate are not visible in the spectrum. No Au 4f signal from the substrate could be measured, even at higher photon energy, consistent with a continuous and thick polymeric film of about 100 nm, as evaluated by atomic force microscopy. The more prominent spectral features in the various spectra have been labeled from b1 to b6.

Similarly to Figure 1, the DOS and PDOS of several possible reaction products are included in Figure 2. The alignment of

dx.doi.org/10.1021/jp304758b | J. Phys. Chem. C 2012, 116, 15010−15018

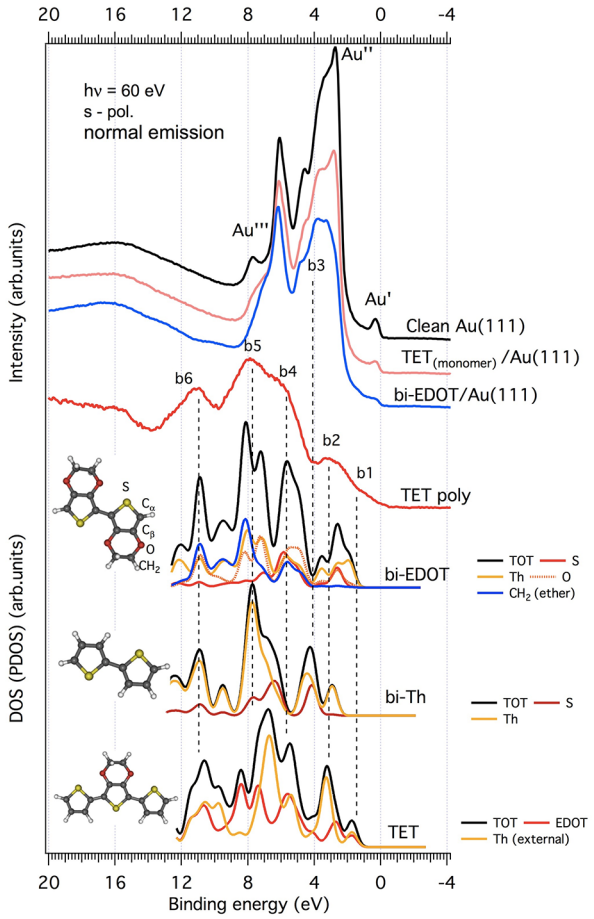

Figure 2. Valence band photoemission spectra of clean Au(111), $TET_{(monomer)}$/Au(111), bi-EDOT/Au(111), and TET polymer. The DOS (PDOS) of bi-EDOT, bithiophene, and TET monomer are shown for comparison.

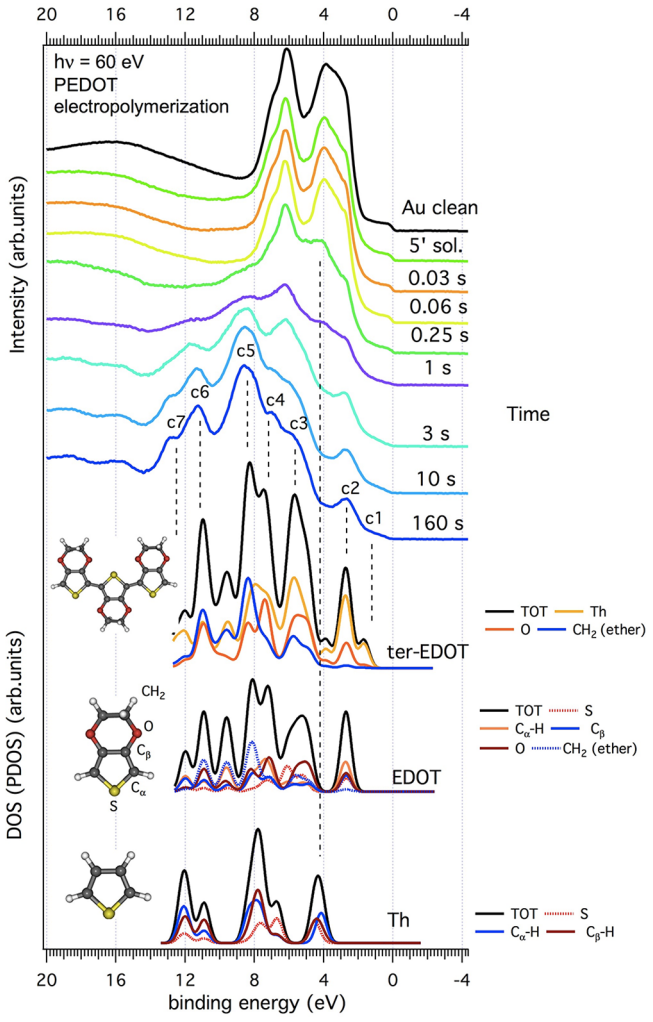

Figure 3. Evolution of valence band photoemission spectra during PEDOT electro-generation process on Au. The DOS (PDOS) of the EDOT trimer, EDOT, and thiophene are shown.

the TET DOS energy scale was obtained by comparison with the TET polymer spectrum.

The evolution of the valence band spectra during the electropolymerization of a PEDOT film on Au is shown finally in Figure 3. The second curve from the top refers to the sample that has been immersed in the EDOT solution for 5 min and then inserted into the electrochemical cell containing only the supporting electrolyte. The following spectra refer to different increasing polymerization times. Larger polymerization times result in a higher thickness of the corresponding film.[29] It has been shown that the film thickness increases almost linearly with the electrogeneration time, passing from 2 Å for 0.03 s to 120 nm for 160 s.[29] Spectral features characteristic of the thick PEDOT film have been labeled c1−c7. At initial deposition stages the valence band is only slightly modified, with a reduction of the structure at about 2.7 eV and with an increasing emission at about and above 8 eV.

Once more, several DOS (PDOS) of relevant molecular systems to be compared to the experimental curves are included in the figure.

NEXAFS. NEXAFS is known as a powerful tool not only for the investigation of the empty electronic levels of a molecular system (in the presence of a core hole), but also because of the possible determination of the orientation of molecules or functional groups at surfaces. This is realized by exploiting the directionality of the dipole transitions with respect to the orientation of the electric field vector of the impinging light.[53]

In Figure 4 (d) and (e) we report the carbon K-edge NEXAFS spectra of bi-EDOT and TET monomer deposited on Au(111) from the vapor phase. The two spectra were recorded in s- and p- light scattering conditions, i.e., with the electric field vector perpendicular and parallel to the scattering plane, respectively. More precisely, in the present case s-polarization refers to the electric field parallel to the surface plane and p-polarization to the electric field with a component perpendicular to the surface plane. Differently from the case of EDOT,[29,30] it can be observed that the spectra taken in the two polarizations show pronounced variations of the peak intensities, which can be related to the specific orientation of the molecular species at the surface.

The spectrum of a thick TET polymer film is also shown in Figure 4f. No angular dependence could be measured for the polymer film.

The main features observed in the spectra (labeled from 1 to 4) have been associated to specific transitions from the C 1s levels to empty molecular orbitals, as discussed in the next section.

Similarly to what has been done for valence band photoemission, for a better assignation of the experimental

dx.doi.org/10.1021/jp304758b | J. Phys. Chem. C 2012, 116, 15010−15018

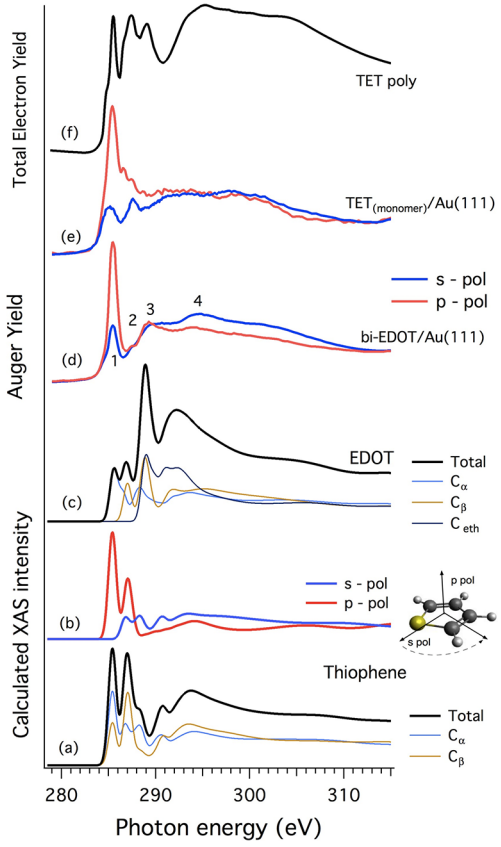

Figure 4. Calculated carbon K edge NEXAFS spectra: (a) thiophene with contributions from nonequivalent centers; (b) thiophene with the electric field perpendicular (p-pol) and parallel (s-pol) to the ring plane; (c) EDOT with contributions from nonequivalent carbon atoms. Experimental spectra of (d) bi-EDOT/Au(111) and (e) $TET_{(monomer)}$/Au(111) deposited from the vapor phase and recorded in Auger yield in s- and p- scattering geometries. (f) Experimental spectrum of a TET polymer measured in total electron yield.

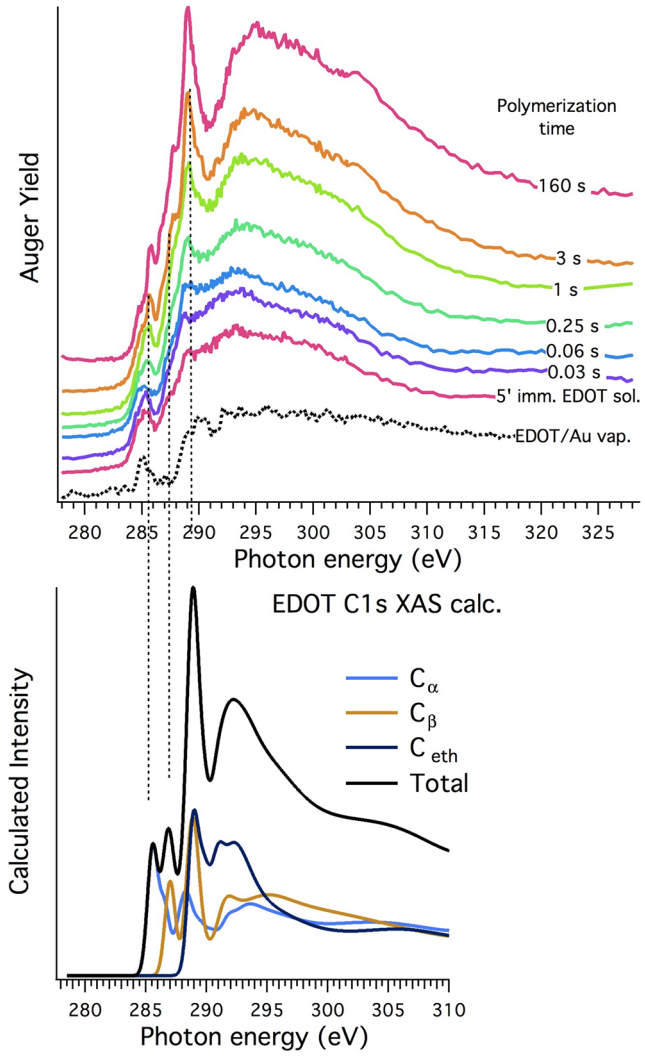

Figure 5. Evolution of the NEXAFS C 1s spectra during PEDOT electro-generation on Au as a function of polymerization time. The spectrum acquired on EDOT deposited on Au(111) from the vapor phase[30] is reported for comparison (dotted line). The calculated X-ray absorption spectrum of the EDOT monomer is also reported in the lower panel. The contributions of the nonequivalent C atoms are highlighted.

features, calculations of the X-ray absorption spectra of isolated thiophene and EDOT have been performed, as shown in Figure 4a–c. Transitions originating from the different C atoms in the molecules are shown separately in the calculated curves of thiophene (Figure 4a) and EDOT (Figure 4c). Concerning thiophene, in Figure 4b calculated polarization dependent spectra are reported. The p- polarization curve refers to the theoretical spectrum obtained with the electric field perpendicular to the ring plane, the s- polarization curve refers to the average spectrum obtained by integration over all directions of the electric field parallel to the plane of the aromatic ring (sketch in Figure 4).

NEXAFS spectra were also acquired at the different steps of the electro-generation process of the PEDOT film. The experimental curves are shown in Figure 5, as a function of polymerization time. In Figure 5, the lower experimental curve (dotted line) refers to the spectrum of EDOT deposited from the vapor phase on clean Au(111), already discussed in ref 30. This is reported here for comparison purposes. The second experimental curve from bottom represents the sample that has been immersed for 5 min in EDOT solution and then inserted in the electrochemical cell containing only the supporting electrolyte.

No angular dependence on the incoming electric field vector was observed. Due to the nature of the polymeric film in electro-generation, a dependence of the signal on the electric field direction is not expected. This holds also at the initial deposition stage and is consistent with the experimental results for EDOT ultrathin layers on polycrystalline Au,[30] where it was not possible to identify any clear linear dichroism.

As a guide in the interpretation of the evolution of the spectral features, the calculated spectrum of EDOT is also reported in Figure 5.

DISCUSSION

Valence Band. The investigation by photoemission of the valence band of ultrathin molecular films on surfaces is often not straightforward. The features from the substrate may dominate the spectrum, making the identification of adsorbate-induced structures not obvious. This is the case of Au, where the intense Au 5d band between 2 and 8 eV binding energy contributes strongly to the electron distribution curves.

Specific calculations of molecular induced levels can be extremely helpful to the correct interpretation of the

dx.doi.org/10.1021/jp304758b | J. Phys. Chem. C 2012, 116, 15010–15018

experimental spectra. The present case is complicated by the fact that the chemisorption of EDOT derivatives may lead to different reaction products at the interface, as observed by core level photoemission and Raman scattering.[29,30] It was found, as a general trend for EDOT derivatives, that chemisorption onto Au results in the loss of the ether group of EDOT, the remaining species being compatible with thiophene or oligothiophene and possibly alkyl chains. In particular, the S 2p core levels present different components that were ascribed[29,30] to thiophene species (at about 163.6 eV of binding energy), possibly in different bonding configurations, to thiolates (at about 162.1 eV) and also to atomic sulfur atoms (at about 161.4 eV) at the Au surface. Correspondingly, the C 1s spectra do not reveal the expected features of C−O bonding, typical of the gas phase EDOT molecule.

For this reason we compared the experimental spectra with the calculated DOS of different possible reaction products that can be present simultaneously at the interface.

Clearly, the DOS of a single molecule does not represent the realistic adsorption situation, since it does not take into account the interaction with the substrate and with the other adjacent molecules chemisorbed at the surface. These effects can be relevant.[54,55] Nevertheless, it is recognized that the main character of the molecular orbitals is generally maintained after chemisorption. Moreover, in the present case, the exact nature of the interface is not uniquely defined. In this sense, the comparison with the DOS of (isolated) single molecules and oligomers is a reasonable compromise for the analysis of the experimental valence bands. For the same reasons, in the calculation of the DOS of the possible oligomers we stopped at three molecular units (trimers of EDOT and thiophene). In many cases it has been shown that this already accounts for the main character shared by longer chains or even by the relevant polymers.[48,50,56]

The comparison between the valence bands of EDOT deposited from the vapor phase and from solution (Figure 1) was already qualitatively discussed in one of our previous works.[30] The *effective* thickness of the molecular layer was evaluated as being extremely small, namely 2 and 3 Å for the film prepared from the vapor phase and from the solution respectively.[30] This means that in both situations the film is extremely thin. In this sense it is not surprising that the Au valence band emission still dominates the spectra. The spectral features of the film prepared in solution appear generally broader, which is related to a higher degree of disorder of the molecular layer and/or to different adsorption sites with respect to the vapor deposition case. This is also consistent with a higher broadening of the S 2p levels for the film prepared in solution, as shown elsewhere.[27,30] Apart from the fact that a slightly higher thickness was found for the film prepared in solution, which justifies the more intense emission from interface related structures, some spectral features could also be ascribed to some residual interface carbonaceous contamination, which was observed to be present on the polycrystalline substrates.[29,30]

On the basis of the comparison with calculated DOS, some considerations on the reaction products can be drawn. Features a1 and a3−a7 in Figure 1 can be associated to the EDOT molecular orbitals, even if the contributions from the ether units (−O−CH_2−CH_2−O−) seem extremely weak in the film prepared from vapor deposition. This is consistent with the fragmentation of the molecule upon adsorption, with the scission of the $C_{aromatic}$−O bonds and the loss of the −O−CH_2−CH_2−O− groups.[29,30] On the other hand, feature a2 does not find correspondence in EDOT. Instead it can be nicely associated to the thiophene−oligothiophene structures that are related to the S sites and to the aromatic rings. a1 is also compatible with oligothiophene orbitals, in particular with π-type states localized on the C atoms of the thiophene rings. The assignation of structures a3−a7 is more complicated, since different molecular groups contribute in this energy interval. Alkyl chain orbitals on CH_2 and CH_3 segments also show their major spectral weight in this region. Here, butanethiol was chosen for comparison with the experiment, since it represents the prototypical reaction product from the opening of a thiophene ring after dissociation. Also the presence of shorter or longer chains or double bonds in the molecules that derive from the ring-opening is possible.

The valence band of TET and bi-EDOT from the vapor phase (Figure 2) is very similar to the case of EDOT. The main relevant feature is b3, which does not correspond well with any of the EDOT derived molecules but can be related to the π-type states of the thiophene rings. Also the weak structure below the Fermi energy can be associated to π-type related states of oligothiophenes (i.e., terthiophene), similarly to feature a1 in Figure 1. The persistence of the surface states of Au(111) for TET could suggest that areas at the surface remain uncovered and maintain their original structure. Alternatively, this could be interpreted in terms of a very weak molecule−substrate interaction, as observed for ultrathin perylene-based molecules on Au.[57] We tend to reject this explanation in the present case, since an evident indication of the reaction of the molecules with the substrate was obtained by S 2p photoemission.[29]

The valence band of the TET polymer sample is completely different from the $TET_{(monomer)}$/Au spectrum. In this case, the Au valence band is obscured due to the film thickness. The features of the polymer spectrum find nice agreement with the calculations of the DOS of TET, which also confirms that the main characteristics of the polymer band are already shown by the single monomer. Features b1 and b2 are principally associated to orbitals mainly localized on the thiophene external rings (Th (external)). Features b4−b6 are related both to EDOT and to thiophene derived states.

The main findings are confirmed also for the PEDOT electro-generated film (Figure 3). The thick layer (160 s polymerization time, corresponding to about 120 nm[29]) presents several features c1−c7 that can be related to the bulk polymer. In this case, the EDOT trimer DOS already gives a good approximation of the polymer band. Molecular orbitals localized principally on the aromatic rings contribute to features c1 and c2. c3 and c4 are associated both to thiophene ring states and to molecular orbitals localized on the oxygen sites. The methylene CH_2 units principally contribute to features c5 and c6. Feature c7 is associated to σ-type states on the aromatic ring.

At initial stages of coverage, when the interface is still accessible to the spectroscopic probe (at 0.03−0.25 s polymerization time, corresponding to 2−6 Å of *effective* film thickness[29]), the valence band is very similar to the case presented in Figure 1 (EDOT/Au sol.), where the structure at about 4 eV binding energy is likely associated to thiophene ring orbitals, in molecules that have lost the ether moieties. Emission at high binding energy, at about 8 eV, can be also ascribed to thiophene or oligothiophene related states.

dx.doi.org/10.1021/jp304758b | J. Phys. Chem. C 2012, 116, 15010−15018

The similarity of the two spectra after 5 min dipping time, either without polymerization in EDOT solution or after 0.03 s polymerization time, supports the idea that EDOT reaction products initially deposited at the surface are not desorbed within the first instants of the electro-generation process. This is even more evident in NEXAFS (see below).

NEXAFS. NEXAFS provides complementary information with respect to photoelectron spectroscopy. Similarly to photoemission, the simulation of the NEXAFS spectra of relevant molecules is extremely helpful for the interpretation of the experimental results. The calculated spectrum of thiophene is shown in Figure 4a. The first structure at 285.6 eV is mainly associated to a transition from the carbon in the α position, with a minor contribution from the carbon in the β position. Vice versa, the second peak at 287.2 eV is principally related to β carbon, with a minor weight due to α carbon. Polarization dependent spectra in Figure 4b and comparison with literature[24,58] permit one to associate the first structure to the π_1* resonance and the second to the π_2* resonance with contributions from the $C_\alpha 1s \rightarrow \sigma^*(C-S)$ transition. The structure at about 290 eV and the broad feature at 292−294 eV are associated to $\sigma^*(C-H)$ and $\sigma^*(C-C)$ transitions within the ring plane, respectively.

Concerning the calculated spectrum of EDOT (Figure 4c), the first peak at about 285.6 eV photon energy is related to transitions from the 1s levels of the carbon atoms in the α position to the LUMO state of the molecule, similarly to the case of thiophene. The second peak at 287.2 eV is associated to transitions from the carbons in β positions to the LUMO. The third strong feature at about 289 eV is associated to transitions from the carbon atoms in the ether moieties to π^* C−O states. Higher energy broad transitions are assigned to dipole excitations from the C atoms in the CH_2 groups to $\sigma^*(C-H)$ and $\sigma^*(C-C)$ empty orbitals. The present calculation and assignment are in good agreement with the data presented and discussed by Birgerson et al. for the gas phase monomer.[59]

Due to the "local" nature of the excitation, it can be expected that the main characteristics of the X-ray absorption spectrum of EDOT are shared also by the dimer. The bi-EDOT spectra in Figure 4d clearly do not reproduce the expected line shape of the unperturbed molecule. Considering the possible reaction products suggested by photoemission,[29] the strong resonance (1) at about 285.5 eV can be associated with the transition to the π^*_1 empty states in thiophene rings of single thiophene units[24,25,58] or related oligomers[60,61] that may be formed after the rupture of the original molecule. Feature labeled (2) can be ascribed to the π_2* resonance in thiophene units.

More interestingly, the structure (3) at about 289 eV is not so pronounced as one would expect for EDOT, but it cannot be explained even by considering the thiophene-related $\sigma^*(C-H)$ transition alone. The possible formation of alkyl chains (alkanethiolates) should be taken into account, giving contributions in this spectral region due to transitions to the $\sigma^*(C-H)$ empty states.[62] Moreover, this would also explain the broad and pronounced resonance (4) at about 294.5 eV, associated to $\sigma^*(C-C)$ excitations not only in the thiophene ring, but also in the alkyl chains. The present finding is consistent with the work of Sako et al.,[25] who have previously observed a reactive adsorption of thiophene on Au, with the possible formation of alkanethiolates at the interface. The finding is also in agreement with our earlier NEXAFS study of EDOT monomer chemisorption on Au.[30] While in that case it was not possible to derive any information on the molecular orientation at the surface, in the present case a clear linear dichroism behavior is observed. From the angular dependence (s- and p- spectra) of the most prominent thiophene related resonances it can be inferred that the thiophene/oligothiophene reaction products adopt an almost flat-lying configuration at the interface.

This picture is confirmed also for the $TET_{(monomer)}$ (Figure 4e). In this case, the feature at 289 eV is completely absent, supporting the indication of the loss of the CH_2 units. The first two resonances are assigned to the thiophene π^* states, while the broad feature above 290 eV is ascribed to σ^*-type transitions in thiophene and alkyl reaction products. The observed linear dichroism supports the flat alignment of the thiophene rings with respect to the substrate plane as well.

The situation is different for the thick TET polymer film. The experimental spectrum (Figure 4f) is characterized by three peaked structures at 285.5, 287.4, and 289 eV and a broad shoulder above 290 eV. Taking into account that every TET unit is composed of two thiophene and one EDOT subunits, comparison with calculated spectra of EDOT and thiophene permits one to associate the first two resonances to the thiophene groups (with minor contributions from EDOT) and the third structure to the CH_2 moieties (C_{eth}) in EDOT. This is consistent with the fact that molecular dissociation occurs only at the interface with the metal and does not involve the polymer film.

Regarding the NEXAFS spectra of electro-generated PEDOT (figure 5), the experimental curves show a progressive evolution from the earliest stages of film deposition to the formation of the bulk polymer. Due to the surface sensitivity of the Auger yield acquisition mode, it can be assumed that the first spectra carry information on the interface, which is progressively obscured as the electro-polymerization proceeds.

The spectrum recorded after 5 min of dipping time in EDOT solution and then immersed into the electrochemical cell with only the electrolyte is comparable to the spectrum recorded after 0.03 s of polymerization time and it is very similar to the spectrum of EDOT/Au deposited from the vapor phase. This similarity indicates that the sample produced ex situ is not so different from the "ideal" case, which means that the "ideal" sample (vapor phase deposition, without contamination) is representative for understanding also the realistic, ex situ situation. This suggests also that, as mentioned previously, the molecular layer that is initially adsorbed is not desorbed during the first electro-generation step. It can be observed that by increasing the polymerization time, the spectra progressively evolve, with a prominent feature rising at about 289 eV.

The comparison with calculated X-ray absorption is again crucial for the assignation of the spectral features and molecular recognition.

After a 5 min dipping and at extremely short polymerization times the line shape cannot be related to excitations of the EDOT molecule. Strong similarities are indeed observed with the spectra presented in our previous work for EDOT chemisorption from the vapor phase and from solution[30] and with the case of bi-EDOT. Although some contribution from contaminants on the pristine surface can be present, resonances at 285.5 and 288−289 eV can be associated to thiophene and thiolate reaction products. Only after longer electro-polymerization times a peaked, well-defined feature appears at 289 eV, and a pronounced broad structure emerges at 293−295 eV, which unambiguously can be related to the PEDOT polymer.

CONCLUSIONS

This work extends our previous study[29,30] of the chemisorption of 3,4-ethylenedioxythiophene (EDOT) and some of its relevant derivatives on Au single crystal and polycrystalline surfaces. Photoemission is used to derive information on the valence band of EDOT, of its dimer (bi-EDOT), of 3′,4′-ethylenedioxy-2,2′:5′,2″-terthiophene (TET) and of the PEDOT electro-generated polymer on Au, focusing on the differences between the interface and the bulk polymeric film. The valence bands are dominated by the emission from the substrate 5d band; in order to derive conclusions on the possible reaction products and their related valence band features, the spectra are compared with the calculated DOS of selected molecules. For bi-EDOT, TET, and PEDOT, NEXAFS was performed in addition to the photoemission to obtain complementary information on molecular orientation and reaction products. As a general trend, it is confirmed that the initial chemisorption stages lead to molecular dissociation and possible oligomerization reactions. The reaction products consist of thiophene/oligothiophene species that likely adopt a planar orientation at the interface. In addition, alkyl chains (alkanethiolates) are also possibly formed. The reasons for the disruption reaction at the initial deposition stages are still unclear. Dissociation is possibly related to the role of defects at the surface, grain boundaries and step edges, which act as reaction centers already at room temperature. It should be noted, however, that in this case one would qualitatively expect higher dissociation/reaction levels on polycrystalline surfaces with respect to the single crystal. This is not well evident from our data.

The identification of the reaction mechanism leading to the decomposition of EDOT derivatives on Au represents a challenging task. Au is considered possessing a limited reactivity. However Au, especially in the form of nanoparticles, has been demonstrated to be an effective catalyst in a large number of reactions[63−65]

Investigations carried out in the frame of the hydrodesulphurization process can give a rationale to the phenomena occurring on Au. These reactions, in fact, are involved in the refining process of crude oil in order to reduce the environmental impact of the resulting fuels through the removal of sulphurated species, including those based on thiophene.[66−68]

The reaction mechanism is a complex one, since a large number of steps could occur. In particular, the adsorption step can lead to the formation of an η-n adduct, which constitutes a sort of surface complex of thiophene with the metal atoms on the catalyst surface. In addition, the formation of metallocycles has been reported: the metal atom on the surface can be part of a six-atom cycle. The following step leads to the formation of sulfur atom and thiol molecules on the surface and the release of butane and different butenes. The exact nature of the reaction steps strongly depends on the nature of the catalysts and on the experimental conditions. Metal catalysts, typically Ni or W, supported on metal oxides, are often employed for the purpose and similar reactions have been observed on the surface of different metals. Though Au has been reported to be a poor catalyst for the hydrodesulpurization process,[69] it has been recently proposed as a potential cocatalyst in association with other metals.[70,71]

Finally, reaction pathways similar to those described in the case of hydrodesulphurization process have been observed also in the case of metal complexes and organometallic compounds prepared by employing different thiophene derivatives and metals (e.g., Rh and Ir).[67] As to Au, different organometallic compounds based on thiophene derivatives are known,[72] although the reactivity of these metal complexes is relatively poorly investigated.

AUTHOR INFORMATION

Corresponding Author

*E-mail: luca.pasquali@unimore.it.

Notes

The authors declare no competing financial interest.

ACKNOWLEDGMENTS

The experiments were carried out following Proposals 20085440 and 2008489.

REFERENCES

(1) Gooding, J. J.; Ciampi, S. *Chem. Soc. Rev.* **2011**, *40*, 2704−2718.
(2) Prakash, S.; Karacor, M. B.; Banerjee, S. *Surf. Sci. Rep.* **2009**, *64*, 233−254.
(3) Whitesides, G. M.; Love, J. C.; Estroff, L. A.; Kriebel, J. K.; Nuzzo, R. G. *Chem. Rev.* **2005**, *105*, 1103−1169.
(4) Zaera, F.; Ma, Z. *Surf. Sci. Rep.* **2006**, *61*, 229−282.
(5) Hwang, J.; Wan, A.; Kahn, A. *Mater. Sci. Eng. R* **2009**, *64*, 1−31.
(6) Grobosch, M.; Knupfer, M. *Open Appl. Phys. J.* **2011**, *4*, 8−18.
(7) Jung, C.; Dannenberger, O.; Xu, Y.; Buck, M.; Grunze, M. *Langmuir* **1998**, *14*, 1103−1107.
(8) Laibinis, P. E.; Whitesides, G. M.; Allara, D. L.; Tao, Y.-T.; Parikh, A. N.; Nuzzo, R. G. *J. Am. Chem. Soc.* **1991**, *113*, 7152−7167.
(9) Noh, J.; Kato, H. S.; Kawai, M.; Hara, M. *J. Phys. Chem. B* **2006**, *110*, 2793−2797.
(10) Porter, M. D.; Bright, T. B.; Allara, D. L.; Chidsey, C. E. D. *J. Am. Chem. Soc.* **1987**, *109*, 3559−3568.
(11) Tai, Y.; Shaporenko, A.; Rong, H.-T.; Buck, M.; Eck, W.; Grunze, M.; Zharnikov, M. *J. Phys. Chem. B* **2004**, *108*, 16806−16810.
(12) Duwez, A. S. *J. Electron Spectrosc. Relat. Phenom.* **2004**, *134*, 97−138.
(13) Schreiber, F. *Prog. Surf. Sci.* **2000**, *65*, 151−256.
(14) Esaulov, V. A.; Hamoudi, H.; Prato, M.; Dablemont, C.; Cavalleri, O.; Canepa, M. *Langmuir* **2010**, *26*, 7242−7247.
(15) Grizzi, O.; Alarcon, L. S.; Chen, L.; Esaulov, V. A.; Gayone, J. E.; Sanchez, E. A. *J. Phys. Chem. C* **2010**, *114*, 19993−19999.
(16) Pasquali, L.; Terzi, F.; Seeber, R.; Nannarone, S.; Datta, D.; Dablemont, C.; Hamoudi, H.; Canepa, M.; Esaulov, V. A. *Langmuir* **2011**, *27*, 4713−4720.
(17) Pasquali, L.; Terzi, F.; Seeber, R.; Doyle, B. P.; Nannarone, S. *J. Chem. Phys.* **2008**, *128* (1−10), 134711.
(18) Pasquali, L.; Terzi, F.; Zanardi, C.; Pigani, L.; Seeber, R.; Paolicelli, G.; Suturin, S. M.; Mahne, N.; Nannarone, S. *Surf. Sci.* **2007**, *601*, 1419−1427.
(19) Clemens, W.; Fix, I.; Ficker, J.; Knobloch, A.; Ullmann, A. *J. Mater. Res.* **2004**, *19*, 1963−1973.
(20) Horowitz, G. *J. Mater. Res.* **2004**, *19*, 1946−1962.
(21) Liu, X.; Knupfer, M.; Huisman, B. H. *Surf. Sci.* **2005**, *595*, 165−171.
(22) Ito, E.; Noh, J.; Hara, M. *Surf. Sci.* **2008**, *602*, 3291−3296.
(23) Liu, G.; Rodriguez, J. A.; Dvorak, J.; Hrbek, J.; Jirsak, T. *Surf. Sci.* **2002**, *505*, 295−307.
(24) Nambu, A.; Kondoh, H.; Nakai, I.; Amemiya, K.; Ohta, T. *Surf. Sci.* **2003**, *530*, 101−110.
(25) Sako, E. O.; Kondoh, H.; Nakai, I.; Nambu, A.; Nakamura, T.; Ohta, T. *Chem. Phys. Lett.* **2005**, *413*, 267−271.
(26) Ito, E.; Noh, J.; Hara, M. *Jpn. J. Appl. Phys.* **2003**, *42*, L852−L855.

(27) Terzi, F.; Seeber, R.; Pigani, L.; Zanardi, C.; Pasquali, L.; Nannarone, S.; Fabrizio, M.; Daolio, S. *J. Phys. Chem. B* **2005**, *109*, 19397−19402.
(28) Noh, J.; Ito, E.; Nakajima, K.; Kim, J.; Lee, H.; Hara, M. *J. Phys. Chem. B* **2002**, *106*, 7139−7141.
(29) Terzi, F.; Pasquali, L.; Montecchi, M.; Nannarone, S.; Viinikanoja, A.; Aaritalo, T.; Salomaki, M.; Lukkari, J.; Doyle, B. P.; Seeber, R. *J. Phys. Chem. C* **2011**, *115*, 17836−17844.
(30) Pasquali, L.; Terzi, F.; Montecchi, M.; Doyle, B. P.; Lukkari, J.; Zanfrognini, B.; Seeber, R.; Nannarone, S. *J. Electron Spectrosc. Relat. Phenom.* **2009**, *172*, 114−119.
(31) Kirchmeyer, S.; Reuter, K. *J. Mater. Chem.* **2005**, *15*, 2077−2088.
(32) Zanardi, C.; Terzi, F.; Pigani, L.; Heras, A.; Colina, A.; Lopez-Palacios, J.; Seeber, R. *Electrochim. Acta* **2008**, *53*, 3916−3923.
(33) Zhu, Y. B.; Wolf, M. O. *J. Am. Chem. Soc.* **2000**, *122*, 10121−10125.
(34) Nannarone, S.; Borgatti, F.; DeLuisa, A.; Doyle, B. P.; Gazzadi, G. C.; Giglia, A.; Finetti, P.; Mahne, N.; Pasquali, L.; Pedio, M.; et al. *AIP Conf. Proc.* **2004**, *705*, 450−453.
(35) Pasquali, L.; DeLuisa, A.; Nannarone, S. *AIP Conf. Proc.* **2004**, *705*, 1142−1145.
(36) StoBe-deMon version 3.0; Hermann, K.; Pettersson, L. G. M.; Casida, M. E.; Daul, C.; Goursot, A.; Koester, A.; Proynov, E.; St-Amant, A.; Salahub, D. R. 2007.
(37) Hammer, B.; Hansen, L. B.; Nørskov, J. K. *Phys. Rev. B* **1999**, *59*, 7413−7421.
(38) Perdew, J. P.; Burke, K.; Ernzerhof, M. *Phys. Rev. Lett.* **1996**, *77*, 3865−3868.
(39) Godbout, N.; Salahub, D. R.; Andzelm, J.; Wimmer, E. *Can. J. Chem.* **1992**, *70*, 560−571.
(40) Slater, J. C.; Loewdin, P. O. *Adv. Quantum Chem.* **1972**, 1.
(41) Slater, J. C.; Johnson, K. H. *Phys. Rev. B* **1972**, *5*, 844−853.
(42) Cavalleri, M.; Odelius, M.; Nordlund, D.; Nilsson, A.; Pettersson, L. G. M. *Phys. Chem. Chem. Phys.* **2005**, *7*, 2854−2858.
(43) Kolczewski, C.; Puttner, R.; Plashkevych, O.; Agren, H.; Staemmler, V.; Martins, M.; Snell, G.; Schlachter, A. S.; Sant'Anna, M.; Kaindl, G.; et al. *J. Chem. Phys.* **2001**, *115*, 6426−6437.
(44) Zimmer, H. G.; Goldmann, A.; Courths, R. *Surf. Sci.* **1986**, *176*, 115−124.
(45) Kevan, S. D.; Gaylord, R. H. *Phys. Rev. B* **1987**, *36*, 5809−5818.
(46) Birgerson, J.; Keil, M.; Denier van der Gon, A. W.; Crispin, X.; Logdlund, M.; Salaneck, W. R. *MRS Proc.* **2000**, *660* (1−6), JJ5.29.
(47) Osikowicz, W.; Friedlein, R.; de Jong, M. P.; Sorensen, S. L.; Groenendaal, L.; Salaneck, W. R. *New J. Phys.* **2005**, *7* (1−14), 104.
(48) Osikowicz, W.; van der Gon, A. W. D.; Crispin, X.; de Jong, M. P.; Friedlein, R.; Groenendaal, L.; Fahlman, M.; Beljonne, D.; Lazzaroni, R.; Salaneck, W. R. *J. Chem. Phys.* **2003**, *119* (1−6), 10415.
(49) Chandekar, A.; Whitten, J. E. *Synth. Met.* **2005**, *150*, 259−264.
(50) Fujimoto, H.; Nagashima, U.; Inokuchi, H.; Seki, K.; Cao, Y.; Nakahara, H.; Nakayama, J.; Hoshino, M.; Fukuda, K. *J. Chem. Phys.* **1990**, *92*, 4077−4092.
(51) Duwez, A. S.; DiPaolo, S.; Ghijsen, J.; Riga, J.; Deleuze, M.; Delhalle, J. *J. Phys. Chem. B* **1997**, *101*, 884−890.
(52) Duwez, A. S.; Pfister-Guillouzo, G.; Delhalle, J.; Riga, J. *J. Phys. Chem. B* **2000**, *104*, 9029−9037.
(53) Stohr, J. *NEXAFS Spectroscopy*; Springer: Berlin, 1992; Vol. *25*.
(54) de Oteyza, D. G.; Silanes, I.; Ruiz-Oses, M.; Barrena, E.; Doyle, B. P.; Arnau, A.; Dosch, H.; Wakayama, Y.; Ortega, J. E. *Adv. Funct. Mater.* **2009**, *19*, 259−264.
(55) Loli, L. N. S.; Hamoudi, H.; Gayone, J. E.; Martiarena, M. L.; Sanchez, E. A.; Grizzi, O.; Pasquali, L.; Nannarone, S.; Doyle, B. P.; Dablemont, C.; et al. *J. Phys. Chem. C* **2009**, *113*, 17866−17875.
(56) Xing, K. Z.; Fahlman, M.; Chen, X. W.; Inganas, O.; Salaneck, W. R. *Synth. Met.* **1997**, *89*, 161−165.
(57) de Oteyza, D. G.; Barrena, E.; Ruiz-Oses, M.; Silanes, I.; Doyle, B. P.; Ortega, J. E.; Arnau, A.; Dosch, H.; Wakayama, Y. *J. Phys. Chem. C* **2008**, *112*, 7168−7172.
(58) Hitchcock, A. P.; Tourillon, G.; Garrett, R.; Williams, G. P.; Mahatsekake, C.; Andrieu, C. *J. Phys. Chem.* **1990**, *94*, 2327−2333.
(59) Birgerson, J.; Keil, M.; Luo, Y.; Svensson, S.; Agren, H.; Salaneck, W. R. *Chem. Phys. Lett.* **2004**, *392*, 100−104.
(60) Koller, G.; Blyth, R. I. R.; Sardar, S. A.; Netzer, F. P.; Ramsey, M. G. *Surf. Sci.* **2003**, *536*, 155−165.
(61) Okajima, T.; Narioka, S.; Tanimura, S.; Hamano, K.; Kurata, T.; Uehara, Y.; Araki, T.; Ishii, H.; Ouchi, Y.; Seki, K.; et al. *Jpn. J. Appl. Phys. 1* **1996**, *35*, 2822−2825.
(62) Dannenberger, O.; Weiss, K.; Himmel, H. J.; Jager, B.; Buck, M.; Woll, C. *Thin Solid Films* **1997**, *307*, 183−191.
(63) Corti, C. W.; Holliday, R. J.; Thompson, D. T. *Top. Catal.* **2007**, *44*, 331−343.
(64) Gong, J. *Chem. Rev.* **2012**, *112*, 2987−3054.
(65) Bond, G. C.; Louis, C.; Thompson, D. T. *Catalysis by gold*; Imperial College Press: London, 2006.
(66) Friend, C. M.; Chen, D. A. *Polyhedron* **1997**, *16*, 3165−3175.
(67) Sánchez-Delgado, R. A. *Organometallic modeling of the hydrodesulfurization and hydrodenitrogenation reactions*; Kluwer Academic Publishers: New York, 2002.
(68) Stirling, D. *The sulfur problem: cleaning up industrial feedstocks*; The Royal Society of Chemistry: Cambridge, U.K., 2000.
(69) Pecoraro, T. A.; Chianelli, R. R. *J. Catal.* **1981**, *67*, 430−445.
(70) Griffe, B.; Brito, J. L.; Sierraalta, A. *J. Mol. Catal. A: Chem.* **2010**, *315*, 28−34.
(71) Suo, Z. H.; Lv, A. H.; Lv, H. Y.; Jin, M. S.; He, T. *Catal. Commun.* **2009**, *10*, 1174−1177.
(72) Porter, K. A.; Schier, A.; Schmidbaur, H. *Organometallics* **2003**, *22*, 4922−4927.